

Ferromagnetism in ZnO codoped with transition metals: $Zn_{1-x}(FeCo)_xO$ and $Zn_{1-x}(FeCu)_xO$

Min Sik Park and B. I. Min

Department of Physics and Electron Spin Science Center, Pohang University of Science and Technology, Pohang 790-784, Korea

(Received 15 July 2003; published 31 December 2003)

We have investigated electronic structures and magnetic properties of ZnO-based potential diluted magnetic semiconductors codoped with transition metals: $Zn_{1-x}(FeCo)_xO$ and $Zn_{1-x}(FeCu)_xO$. We have found that the origin of the observed ferromagnetism in $Zn_{1-x}(FeCo)_xO$ would be different from that in $Zn_{1-x}(FeCu)_xO$. $Zn_{1-x}(FeCo)_xO$ does not have a tendency to form the Fe-O-Co ferromagnetic cluster, and so the double-exchange mechanism will not be effective. In contrast, $Zn_{1-x}(FeCu)_xO$ has a tendency to form the Fe-O-Cu ferromagnetic cluster with the charge transfer between Fe and Cu, which would lead to the ferromagnetism via a type of the double-exchange mechanism. The ferromagnetic and nearly half-metallic ground state is obtained for $Zn_{1-x}(FeCu)_xO$.

DOI: 10.1103/PhysRevB.68.224436

PACS number(s): 75.50.Pp, 71.22.+i, 75.50.Dd

I. INTRODUCTION

“Spintronics,” namely, electronics utilizing the spin degree of freedom of electrons becomes an important emerging field. Spintronics is expected to overcome the limits of traditional microelectronics.¹ Diluted magnetic semiconductors (DMS’s) will play an important role in spintronics as semiconductors do in electronics because of their easy integration into existing electronic devices. Two types of DMS families have been well studied: II-VI type such as Mn-doped CdTe and ZnSe (Ref. 2), and III-V type such as Mn-doped GaAs (Ref. 3). In particular, the latter attracts great attention, because it becomes a ferromagnetic (FM) DMS having the Curie temperature $T_C \sim 110$ K. Recent research effort has been focused on developing new FM-DMS’s operating at room temperature.^{4–9}

Along this line, attempts have been made to fabricate ZnO-based DMS. ZnO is a wide-gap ($E_g \sim 3.44$ eV) II-VI semiconductor, and so it can be used for ultraviolet light-emitting devices. Jin *et al.*¹⁰ fabricated 3d transition metal (TM) doped epitaxial ZnO thin films using the combinatorial laser molecular-beam epitaxy method. They have not detected any indication of ferromagnetism. In contrast, for $Zn_{1-x}Co_xO$ films made by using the pulsed-laser deposition technique, Ueda *et al.*¹¹ observed the FM behavior with T_C higher than room temperature. The reproducibility, however, was less than 10%. Hence the realization of the FM long-range order in Co-doped ZnO films is controversial.

On the other hand, there were also trials to make ZnO-based DMS by doping double TM elements: (Fe,Co) or (Fe,Cu). Cho *et al.*¹² observed the room-temperature ferromagnetism for $Zn_{1-x}(Fe_{0.5}Co_{0.5})_xO$ films fabricated by using the reactive magnetron co-sputtering technique. The samples seem to have the single phase of the same wurtzite structure as pure ZnO up to $x=0.15$, and the rapid thermal annealing under vacuum leads to increases in T_C , magnetization, and the carrier concentration. Han *et al.*¹³ also observed the ferromagnetism for $Zn_{1-x}(Fe_{1-y}Cu_y)_xO$ bulk samples with $T_C \sim 550$ K. The bulk sample has the advantage of insensitivity to the detailed process conditions, compared to the film sample fabricated under the nonequilibrium conditions. They

observed the saturation magnetic moment of $0.75 \mu_B$ per Fe, which increases as the Cu-doping ratio increases up to 1%. In addition, the large magnetoresistance was observed below 100 K.

Motivated by these experimental reports on the FM ZnO codoped with transition metals, we have studied electronic structures and magnetic properties of (Fe,Co) and (Fe,Cu) doped ZnO: $Zn_{0.875}(Fe_{0.5}M_{0.5})_{0.125}O$ ($M = Co$ or Cu). We have used the linearized muffin-tin orbital (LMTO) band method in the local spin-density approximation (LSDA). To explore the effects of the Coulomb correlation U and the spin-orbit (SO) interaction, we have also employed the LSDA+ U +SO method by incorporating U and the SO interaction.¹⁴ ZnO has the wurtzite structure in which anions and cations form the hexagonal close-packed lattices. The wurtzite ZnO is composed of tetrahedrons formed by four O anions. For $Zn_{0.875}(Fe_{0.5}M_{0.5})_{0.125}O$, we have considered an orthorhombic supercell containing sixteen formula units in the primitive unit cell by replacing two Zn atoms by Fe and M atoms ($Zn_{14}Fe_1M_1O_{16}$). For the lattice constants, we assumed those of pure ZnO with $a=6.4998$, $b=11.2580$, $c=5.2066$ Å.

II. ZnO, Fe- AND Co-DOPED ZnO

First, we have checked the electronic structure of pure wurtzite ZnO without doping elements. The overall band structure of the present LMTO result is consistent with existing results.^{15–17} As usual in the LSDA calculations, the obtained energy gap ~ 0.7 eV is only about 20% of the experimental value. Also the position of Zn 3d band (-3.0 – -5.0 eV with respect to the valence-band top) is much shallower than the Zn 3d spectrum obtained by photoemission experiment (~ -9.0 eV).¹⁸ The LSDA+ U band method improves the results of the LSDA, but not so satisfactorily. As shown in Fig. 1, the LSDA+ U calculation yields the increased energy gap (~ 1.0 eV) and the deeper Zn 3d band (-6.0 – -7.0 eV). The LSDA+ U result for the Zn 3d position is consistent with result obtained by the GW band calculation.^{16,17} Still the energy gap and Zn 3d position are smaller and shallower than experimental values.

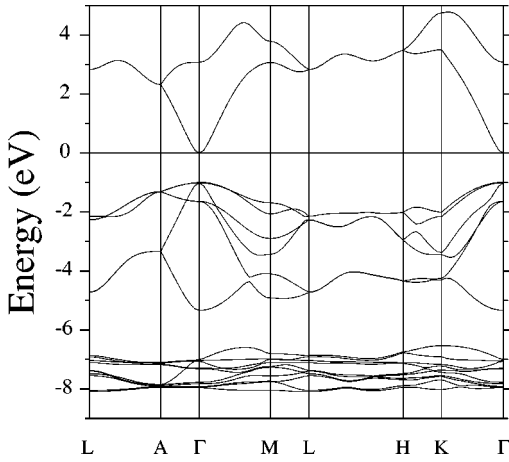


FIG. 1. The LSDA+ U band structure of ZnO with $U=3.0$ eV for Zn 3d electrons. The lowest and intermediate bands correspond to mainly Zn 3d and O 2p bands, respectively. Zn 3d bands in the LSDA are too shallow to become mixed with O 2p bands.

We then have performed the LSDA band calculations for Fe- and Co-doped ZnO: $\text{Zn}_{1-x}\text{Fe}_x\text{O}$ and $\text{Zn}_{1-x}\text{Co}_x\text{O}$ ($x=0.0625$). Due to heavy computational load in the supercell calculations for doped ZnO systems, we have not considered the Coulomb correlation U for Zn 3d electrons.¹⁹ Sato and Yoshida⁵ have reported electronic structures of ZnO doped with TM elements for 25% TM doping concentration by using the Korringa-Kohn-Rostoker band method combined with the coherent potential approximation. They found that V-, Cr-, Fe-, Co-, and Ni-doped ZnO would have the FM ground states rather than the spin-glass states. With this background, we thus consider below only the FM states for Fe- and Co-doped ZnO with more realistic TM doping concentration of 6.25%.

Figure 2 shows the LSDA total density of states (DOS) and TM 3d projected local DOS (PLDOS) for $\text{Zn}_{0.9375}\text{Fe}_{0.0625}\text{O}$ and those for $\text{Zn}_{0.9375}\text{Co}_{0.0625}\text{O}$. For both Fe- and Co-doped ZnO, we have obtained nearly *half-metallic* electronic structures, that is, the conduction electrons at the Fermi level E_F are almost 100% spin polarized. The minority spin 3d states of both Fe and Co near E_F are seen to be hybridized slightly with the conduction band (see Fig. 3). Both for Fe-doped and Co-doped ZnO, the Fermi level cuts the sharp minority spin e states. Note that Fe and Co ions are located at the centers of tetrahedra formed by O ions, and so the e states are lower in energy than the t_2 states. Since there is nearly one more d electron in Co-doped ZnO, the Fermi level is located near the valley between the Co e and t_2 minority spin states. The exchange splittings are larger than the crystal-field splittings, reflecting the high-spin states of Fe and Co in ZnO. Especially, the exchange splitting in Fe-doped ZnO is very large to locate both the e and t_2 states deep in energy, and so the majority spin Fe t_2 states become fully hybridized with O 2p states to yield a broad band. In contrast, the t_2 states in Co-doped ZnO are shallow and located above the O 2p valence band and so the hybridization becomes weak.

The total magnetic moments $4.44 \mu_B$ and $3.25 \mu_B$ for Fe- and Co-doped ZnO come mostly from Fe ($4.11 \mu_B$) and Co

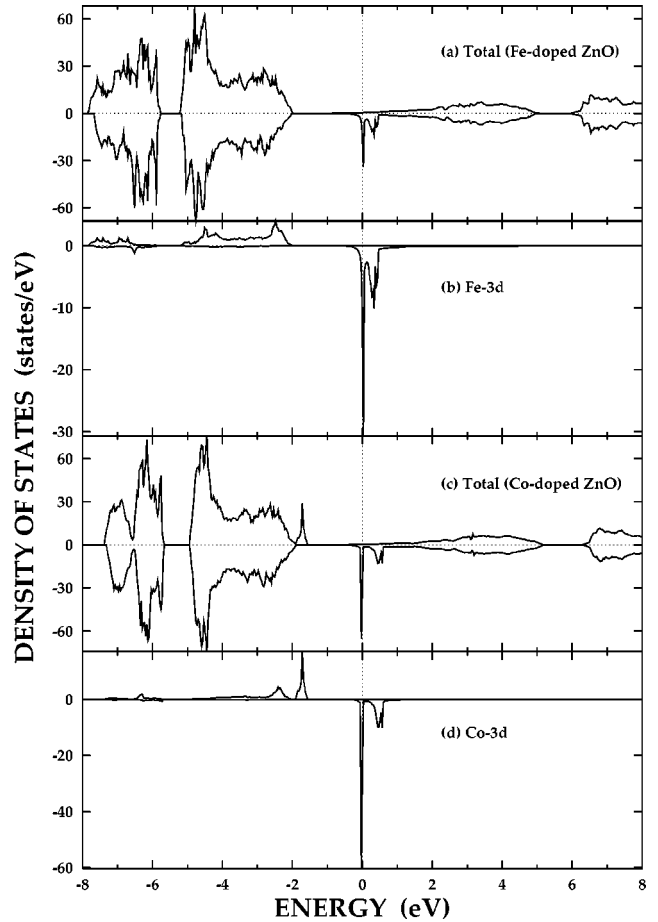


FIG. 2. The LSDA total and TM 3d PLDOS's of $\text{Zn}_{0.9375}\text{Fe}_{0.0625}\text{O}$ and $\text{Zn}_{0.9375}\text{Co}_{0.0625}\text{O}$.

($2.92 \mu_B$) ions, respectively. These results suggest electron occupancies of d^6 (Fe^{2+}) and d^7 (Co^{2+}), respectively. Figure 3 provides the band structure of $\text{Zn}_{0.9375}\text{Co}_{0.0625}\text{O}$ near E_F . The size of circle in the figure represents the amount of Co 3d component in the wave function. It is seen that the rather flat majority spin Co 3d states are located below the Zn 4s conduction band by ~ 1.0 eV. The minority spin Co 3d states are located near and above E_F manifesting hybridization with the Zn 4s conduction-band states. However, we do not expect that either Fe- or Co-doped ZnO in nature has a stable metallic FM ground state, as obtained above. The high DOS's at E_F for both Fe- and Co-doped ZnO would drive the possible structural instability or become reduced substantially by the Coulomb correlation interaction between TM 3d electrons. Indeed, the LSDA+ U band calculation with $U=5.0$ eV for Co 3d electrons yields the insulating ground state for Co-doped ZnO, distinctly from the LSDA band results.²⁰

III. (Fe,Co) DOPED ZnO

Now we have performed the LSDA band calculations for (Fe,Co) doped ZnO: $\text{Zn}_{1-2x}\text{Fe}_x\text{Co}_x\text{O}$ ($x=0.0625$). We have examined magnetic properties by varying the separation between Fe and Co in the supercell: 3.2499, 5.6055, and 6.4998

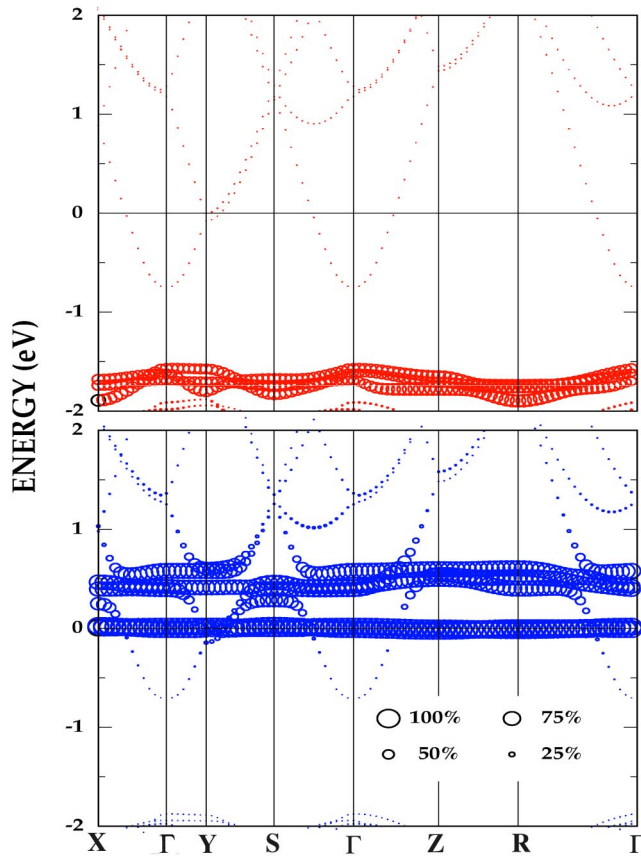


FIG. 3. Band structure of $\text{Zn}_{0.9375}\text{Co}_{0.0625}\text{O}$ near the Fermi level (the upper panel for the majority and the lower panel for the minority spin band). The size of circle represents the amount of Co $3d$ component in the wave function.

\AA . 3.2499 \AA corresponds to a nearest Fe-Co separation with Fe-O-Co configuration in the a - b plane of the orthorhombic supercell, while 5.6055 and 6.4998 \AA to farther Fe-Co separations with Fe-O-Zn-O-Co configurations along the diagonal direction and in the a - b plane, respectively. Total energies are nearly the same among three cases: the shortest 3.2499 \AA case has the lowest total energy by only ~ 3 mRy. This result reflects that there will not be any noticeable TM clustering effect in the (Fe,Co) doped ZnO. Further, for all three cases, we have found that the FM configuration of Fe and Co spins is found to be slightly more stable than the antiferromagnetic (AFM) configuration. For a Fe-Co separation of 5.6055 \AA , the energy difference amounts to ~ 3 mRy.

Figure 4 shows the LSDA DOS of $\text{Zn}_{0.875}\text{Fe}_{0.0625}\text{Co}_{0.0625}\text{O}$ for a Fe-Co separation of 5.6055 \AA . The Fe and Co $3d$ PLDOS's in the codoped case look very similar to those of the single TM-doped cases of Fig. 2. There is no indication of charge transfer between Fe and Co, and so Fe^{2+} and Co^{2+} valence configurations are retained in the (Fe,Co) doped ZnO. This suggests that the *double-exchange* mechanism²¹ will not be effective in $\text{Zn}_{1-2x}\text{Fe}_x\text{Co}_x\text{O}$, because the kinetic-energy gain through the hopping of spin-polarized carriers between Fe and Co ions does not seem to occur. Thus to explain the observed ferromagnetism in $\text{Zn}_{1-2x}\text{Fe}_x\text{Co}_x\text{O}$,¹² one needs to invoke another exchange mechanism between

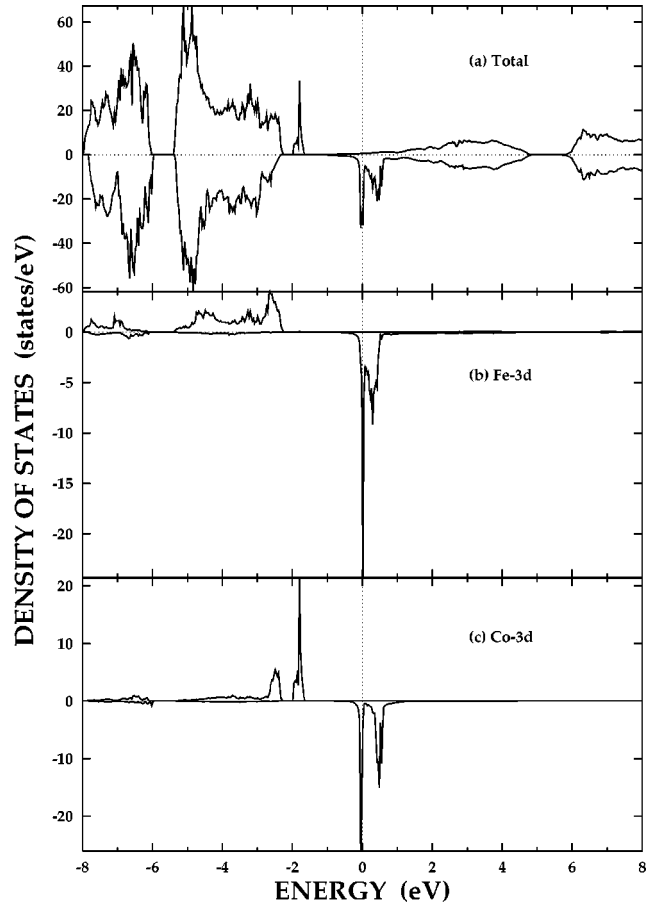


FIG. 4. The LSDA total and TM $3d$ PLDOS's of $\text{Zn}_{0.875}\text{Fe}_{0.0625}\text{Co}_{0.0625}\text{O}$ for a Fe-Co separation of 5.6055 \AA case.

Fe and Co, such as the RKKY-type exchange interaction mediated by Zn $4s$ carriers or conduction carriers induced by oxygen vacancies. In addition, one cannot rule out the formation of separated Fe or Co metallic clusters in $\text{Zn}_{1-2x}\text{Fe}_x\text{Co}_x\text{O}$ which would exhibit the ferromagnetism. Also the possible formation of impurity phases such as spinel CoFe_2O_4 is worthwhile to be checked. These features remain to be resolved more carefully in experiments.

IV. Cu-DOPED ZnO

Before discussing (Fe, Cu) doped ZnO, we have examined electronic structure of Cu-doped ZnO, $\text{Zn}_{0.9375}\text{Cu}_{0.0625}\text{O}$. Interestingly, as shown in Fig. 5, we have obtained the stable FM and half-metallic ground state for Cu-doped ZnO in the LSDA. The total magnetic moment is $1 \mu_B$ and the local moment of Cu is $0.81 \mu_B$, corresponding to the Cu^{2+} (d^9) valence state. The Cu $3d$ PLDOS in Fig. 5(b) indicates that Cu has the DOS of an intermediate spin state. In contrast to Fe- or Co-doped case, the empty Cu $3d$ states are located in the gap region without the hybridization with the Zn $4s$ conduction band, and thus Cu $3d$ states are strongly localized. We presume that this would be the reason why the Cu solubility in ZnO is so low, $\sim 1\%$ at most.

Since the Cu $3d$ states near E_F correspond to partially occupied atomiclike t_2 states, Cu ions would have large or-

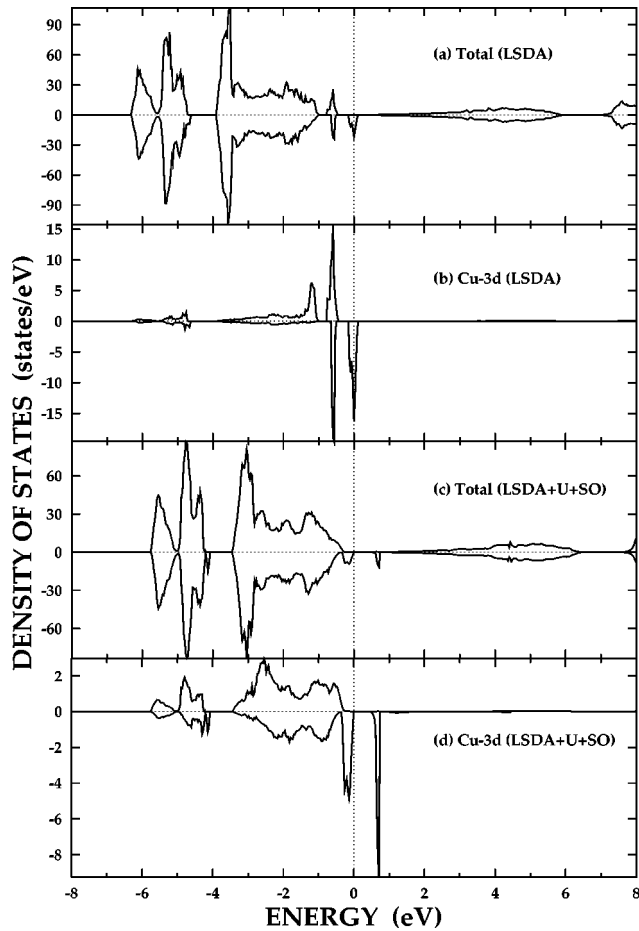


FIG. 5. The LSDA and LSDA + U + SO ($U = 3.0$ eV) total and Cu 3d PLDOS's for $\text{Zn}_{0.9375}\text{Cu}_{0.0625}\text{O}$.

bit magnetic moment. Indeed the LSDA + U + SO calculation yields the substantial orbital magnetic moment of $1.05\mu_B$ with the insulating electronic structure.²² The large orbital moment arises from occupied minority spin t_2 states split by the Coulomb correlation and the spin-orbit interaction.²³ The orbital moment is polarized in parallel with the spin moment, and so the total magnetic moment amounts to $1.85\mu_B/\text{Cu}$.

In general, an ion at the tetrahedral center with low-spin d^9 state would be Jahn-Teller active. In fact, there was a report²⁴ that the account of the dynamical Jahn-Teller effect is necessary to explain the observed paramagnetic susceptibility for Cu-doped ZnO. To examine the Jahn-Teller effect in Cu-doped ZnO, we have considered the local distortion of a tetrahedron around Cu by tilting oxygen ions at the corners. The oxygen ions are tilted by $\sim 13^\circ$ toward the xy plane with retaining Cu-O separations (here xyz coordinates represent the local principle axis). The LSDA band calculation for this system yields a more stable insulating ground state with enhanced spin magnetic moment of $0.99\mu_B/\text{Cu}$. That is, due to the Jahn-Teller distortion, Cu 3d electrons become more localized and the system becomes insulating. The orbital moment in this case would be quenched due to the Jahn-Teller effect.

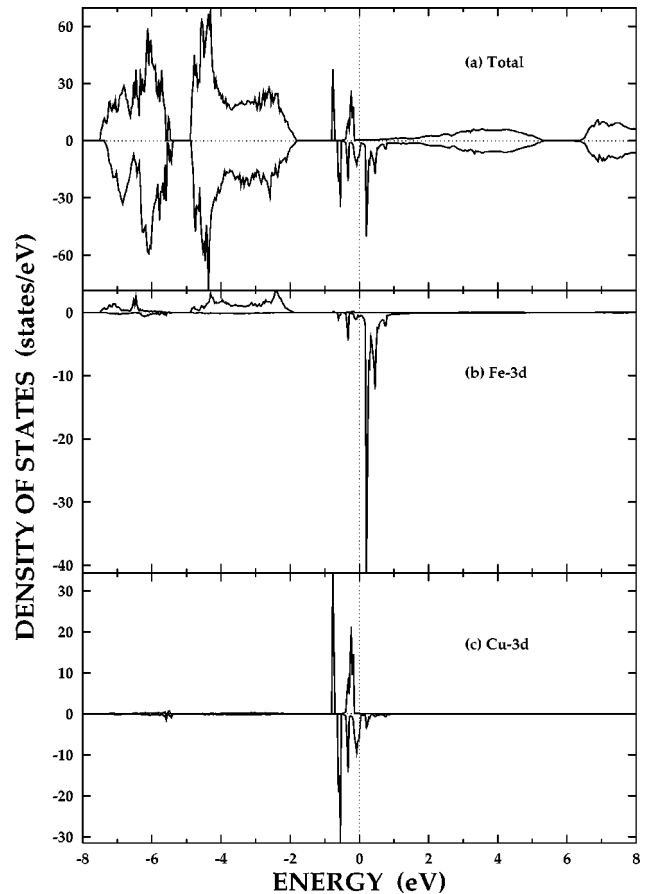


FIG. 6. The LSDA total and TM 3d PLDOS's for $\text{Zn}_{0.875}\text{Fe}_{0.0625}\text{Cu}_{0.0625}\text{O}$ for a Fe-Cu separation of 3.2499 \AA .

V. (Fe, Cu) DOPED ZnO

As is done for (Fe,Co) doped ZnO, we have studied magnetic properties of $\text{Zn}_{1-2x}\text{Fe}_x\text{Cu}_x\text{O}$ ($x = 0.0625$) with varying the separation between Fe and Cu: 3.2499 , 5.6055 , and 6.4998 \AA . For all three cases, the FM configuration of Fe and Cu spins is found to be more stable than the AFM configuration,²⁵ as for the (Fe,Co) doped case. In contrast to the (Fe,Co) doped case, however, we have found that the configuration with the shortest Fe-Cu separation becomes much more stable with respect to other two cases by ~ 30 mRy. This value of the total energy difference is substantial as compared to ~ 3 mRy difference for the (Fe,Co) doped case. This result indicates that Fe and Cu ions in (Fe, Cu) doped ZnO have a tendency to form the Fe-O-Cu clusters. For 1% Cu-doped $\text{Zn}_{0.95}\text{Fe}_{0.05}\text{O}$ bulk sample, Han *et al.*¹³ observed rather small saturated magnetic moment of $0.75\mu_B$ per Fe. This value corresponds to only about 1/5 of ideal Fe^{2+} local moment $4\mu_B$. Incidentally, the value 1/5 is matched with Cu/Fe doping ratio, suggesting a possibility that the only Fe's forming the Fe-O-Cu clusters would give rise to the FM moment, that is, other Fe ions do not produce the long-range FM order. As shown below, the FM ground state in (Fe,Cu) doped ZnO can be understood based on the enhanced double-exchange-like interaction through the Fe-O-Cu clustering effect.

Figure 6 presents the LSDA DOS of

$\text{Zn}_{0.875}\text{Fe}_{0.0625}\text{Cu}_{0.0625}\text{O}$ for the shortest Fe-Cu separation of 3.2499 Å. Above all, one can notice the strong hybridization between Fe and Cu 3*d* states. Further, it is clearly seen in Fig. 6(c) that some new states emerge in the Cu 3*d* minority spin PLDOS between *e* and *t*₂. The new states have *d*_{xy}-like characters directing toward Fe ions.²⁶ Cu 3*d* PLDOS has a reduced exchange splitting, manifesting the DOS characteristic of the low-spin state. This feature is different from other two configurations with larger Fe-Cu separation, which have an intermediate spin state as in Cu-doped ZnO. For all three cases, the hybridization between Cu 3*d* and the conduction-band exists, which is again distinct from Cu-doped ZnO. Due to this hybridization, the conduction carriers of mostly Zn 4*s* states become reduced. The experimental result of the reduced number of carriers in (Fe,Cu) doped ZnO with respect to that in Fe-doped ZnO (Ref. 13) can be understood in terms of the hybridization between the Cu 3*d* and Zn 4*s* states. Noteworthy from PLDOS's of Fig. 6 is that there occurs charge transfer from Fe to Cu, and accordingly Fe and Cu are likely to have nominal Fe³⁺ (*d*⁵) and Cu¹⁺ (*d*¹⁰) configurations, respectively. As a result, the electron occupancy at Cu site increases, and so Cu has the reduced spin magnetic moment of 0.51μ_B as compared to 0.81μ_B in Cu-doped ZnO. The charge transfer from Fe to Cu is expected to disturb the Jahn-Teller distortion at Cu sites and concomitantly make a system metallic. Further, it will cause the mixed-valent states for Fe (Fe²⁺-Fe³⁺) and Cu (Cu²⁺-Cu¹⁺) ions, and the consequent double-exchange-like interaction is expected to induce the ferromagnetism in (Fe,Cu) doped ZnO.

VI. CONCLUSION

We have investigated electronic structures of (Fe,Co) and (Fe,Cu) doped ZnO together with those of Fe-, Co-, and Cu-doped ZnO. We have also explored the origins of the observed ferromagnetism in $\text{Zn}_{1-x}(\text{FeCo})_x\text{O}$ and $\text{Zn}_{1-x}(\text{Fe}_{1-y}\text{Cu}_y)_x\text{O}$. The single TM-doped systems would not have the stable metallic FM ground states: Fe- and Co-doped ZnO due to the structural instability or the large Coulomb correlation effect, while Cu-doped ZnO due to the Jahn-Teller effect. For $\text{Zn}_{0.875}\text{Fe}_{0.0625}\text{Co}_{0.0625}\text{O}$, we have found no indication of charge transfer between Fe and Co, suggesting that the double-exchange mechanism will not be effective for the ferromagnetism in (Fe,Co) doped ZnO. Therefore one needs to invoke another exchange mechanism between Fe and Co, or to check the possibility of the formation of impurity phases. In contrast, for $\text{Zn}_{0.875}\text{Fe}_{0.0625}\text{Cu}_{0.0625}\text{O}$, there is a tendency to form the Fe-O-Cu clusters so as to give rise to the charge transfer from Fe to Cu ions. The charge transfer causes the mixed-valent states of Fe and Cu, and accordingly a type the double-exchange interaction is expected to induce the ferromagnetism in (Fe, Cu) doped ZnO. The FM and nearly half-metallic ground state is obtained for (Fe, Cu) doped ZnO.

ACKNOWLEDGMENTS

This work was supported by the KOSEF through the eSSC at POSTECH and in part by the KRF (Grant No. KRF-2002-070-C00038). Helpful discussions with Y. H. Jeong, S-J. Han, and J.-S. Kang are greatly appreciated.

-
- ¹S.A. Wolf, D.D. Awschalom, R.A. Buhrman, J.M. Daughton, S. von Molnar, M.L. Roukes, A.Y. Chtchelkanova, and D.M. Treger, *Science* **294**, 1488 (2001).
- ²J.K. Furdyna and J. Kossut, *DMS's, Semiconductor and Semimetals Vol. 25* (Academic, New York, 1988).
- ³H. Ohno, A. Shen, F. Matsukura, A. Oiwa, A. Endo, S. Katsumoto, and Y. Iye, *Appl. Phys. Lett.* **69**, 363 (1996).
- ⁴T. Dietl, H. Ohno, F. Matsukura, J. Cibert, and D. Ferrand, *Science* **287**, 1019 (2000).
- ⁵K. Sato and H.K. Yoshida, *Semicond. Sci. Technol.* **17**, 367 (2002).
- ⁶G.A. Medvedkin, T. Ishibashi, T. Nishi, K. Hayata, Y. Hasegawa, and K. Sato, *Jpn. J. Appl. Phys., Part 2* **39**, L949 (2000).
- ⁷Y. Matsumoto, M. Murakami, T. Shono, T. Hasegawa, T. Fukumura, M. Kawasaki, P. Ahmet, T. Chikyow, S. Koshihara, and H. Koinuma, *Science* **291**, 854 (2001).
- ⁸K. Ando, H. Saito, Z. Jin, T. Fukumura, M. Kawasaki, Y. Matsumoto, and H. Koinuma, *Appl. Phys. Lett.* **78**, 2700 (2001).
- ⁹S. Cho, S. Choi, G.-B. Cha, S.C. Hong, Y. Kim, Y.-J. Zhao, A.J. Freeman, J.B. Ketterson, B.J. Kim, Y.C. Kim, and B.-C. Choi, *Phys. Rev. Lett.* **88**, 257203 (2002).
- ¹⁰Z. Jin, T. Fukumura, M. Kawasaki, K. Ando, H. Saito, T. Sekiguchi, Y.Z. Yoo, M. Murakami, Y. Matsumoto, T. Hasegawa, and H. Koinuma, *Appl. Phys. Lett.* **78**, 3824 (2001).
- ¹¹K. Ueda, H. Tabata, and T. Kawai, *Appl. Phys. Lett.* **79**, 988 (2001).
- ¹²Y.M. Cho, W.K. Choo, H. Kim, D. Kim, and Y. Ihm, *Appl. Phys. Lett.* **80**, 3358 (2002).
- ¹³S.-J. Han, J.W. Song, C.-H. Yang, S.H. Park, J.-H. Park, Y.H. Jeong, and K.W. Rhie, *Appl. Phys. Lett.* **81**, 4212 (2002).
- ¹⁴S.K. Kwon and B.I. Min, *Phys. Rev. Lett.* **84**, 3970 (2000).
- ¹⁵P. Schröer, P. Kruger, and J. Pollmann, *Phys. Rev. B* **47**, 6971 (1993).
- ¹⁶M. Oshikiri and F. Aryasetiawan, *J. Phys. Soc. Jpn.* **69**, 2113 (2000).
- ¹⁷M. Usuda, N. Hamada, T. Kotani, and M. van Schilfgaarde, *Phys. Rev. B* **66**, 125101 (2002).
- ¹⁸M. Ruckh, D. Schmid, and H.W. Schock, *J. Appl. Phys.* **76**, 5945 (1994).
- ¹⁹Since the Zn 3*d* bands in the LSDA are located still deep in energy, the effects of the Zn 3*d* bands on the magnetic properties of TM doped ZnO will be minor.
- ²⁰For Fe-doped ZnO, the LSDA+*U* band calculation with *U* = 5.0 eV does not yield the converged results, probably because of too high DOS at *E_F*. With *U* = 9.0 eV, we can obtain the converged insulating ground state.
- ²¹C. Zener, *Phys. Rev.* **82**, 403 (1951).
- ²²We employed parameter values of *U* = 3.0 eV and *J* = 0.87 eV

(J : exchange parameter) for Cu $3d$ electrons.

²³M.S. Park, S.K. Kwon, and B.I. Min, Phys. Rev. B **65**, 161201(R) (2002).

²⁴W.H. Brumage, C.F. Dorman, and C.R. Quade, Phys. Rev. B **63**,

104411 (2001).

²⁵In this case, the band calculation always converges to the ferromagnetic ground state.

²⁶Here too xyz coordinates represent the local principal axis.